Catalysis Science & Technology

Accepted Manuscript

ROYAL SOCIETY OF CHEMISTRY

www.rsc.org/catalysis

NO_x SCR with decane using Ag-MFI catalysts: On the effect of silver content and co-cation presence

Rui Bartolomeu[a,b,c], Acácio Nobre Mendes[a,b,c], Auguste Fernandes[a], Carlos Henriques[a], Patrick Da Costa[b], M. Filipa Ribeiro[a]*

[a] Centro de Química Estrutural, Instituto Superior Técnico, Universidade de Lisboa, Av. Rovisco Pais, 1049-001 Lisboa, Portugal

[b] Sorbonne Universités, UPMC Univ. Paris 06, UMR 7190, Institut Jean le Rond d'Alembert, F-75005, Paris, France.

[c] CNRS, UMR 7190, Institut Jean le Rond d'Alembert, F-78210, Saint-Cyr l'Ecole, France.

*Corresponding author: filipa.ribeiro@tecnico.ulisboa.pt

Abstract

A series of 4 and 9 wt.% Ag/MFI catalysts were prepared using MFI zeolites containing different co-cations (H^+ and Na^+). The effect of the presence of these co-cations, as well and the silver loading, in the stabilisation of different Ag species was assessed by powder XRD, TEM, H_2-TPR, *in situ* DRS UV-Vis and pyridine adsorption followed by FTIR. The results obtained from all techniques allowed the comparison of the catalysts regarding the distribution and nature of Ag silver species and their catalytic performances for the selective catalytic reduction (SCR) of NO_x, in oxygen excess, using *n*-decane as reductant.

It was observed that for an Ag content of 4 wt.%, the presence of Na^+ does not affect the catalysts activity for N_2 formation, whereas for an Ag content of 9 wt.% it decreases N_2 formation. This negative effect observed in deNO_x reaction can be attributed to the decrease in the amount of oxidised Ag species (Ag^+ and $Ag_n^{\delta+}$) and the predominance of Ag^0 particles in samples containing Na. Furthermore, the absence of exchange-sites in the zeolite structure also led to a complete loss of activity. Hence, exchange-sites are crucial for the stabilisation of Ag species (*e.g.* Ag^+ and $Ag_n^{\delta+}$) that are active for the NO_x SCR reaction with *n*-decane.

Keywords: Silver, MFI zeolite, HC-SCR, *n*-decane.

1. Introduction

In an effort to improve the air quality in Europe, the European Union has increased recently the severity of the European Emission Standards (Euro Standards) [1]. These standards apply to vehicles, either with positive-ignition engine (typically, for gasoline) or compress-ignition engine (typically, diesel-powered), and limit maximum emissions of CO, HC, PM (particulate matter) and NO_x.

NO_x emissions in both heavy-duty diesel and passenger vehicles have been specially targeted in the last years, with a decrease from 2.0 to 0.40 g/kWh in January 2013 (Euro VI Standard) and from 0.18 to 0.08 g/kWh in September 2014 (Euro VI Standard), respectively.

Although diesel vehicles NO_x emissions can be achieved by limiting the amount of NO_x produced in the engine, this strategy needs to be applied in conjunction with catalytic after-treatment systems. The two main technologies currently in place by car manufacturers are the Lean NO_x Trap (LNT) and Selective Catalytic Reduction with NH_3 (NH_3-SCR), which can even be used simultaneously to achieve a greater NO_x reduction efficiency [2].

However, both these technologies have different limitations and problems that remain unresolved (*e.g.* LNT thermal and sulphur deactivation, and NH_3-SCR ammonia slip). In order to overcome these issues, a technology which has been studied over the last 20 years, Selective Catalytic Reduction with Hydrocarbons (HC-SCR), may be an interesting alternative. The main reaction of HC-SCR is described by Equation (1), with C_xH_y being the HC reductant.

$$2\,NO + C_xH_y + \left(x + \frac{y}{4} - 1\right) O_2 \rightarrow N_2 + x\,CO_2 + \frac{y}{2}\,H_2O \qquad (1)$$

Therefore, this technology employs HC molecules that can be already present in the exhaust gases or that can be obtained from fuel injection on the exhaust gases coming from the engine. In this way, the requirement of an additional urea tank, feed system and all problems associated with ammonia slip can be avoided.

The use of silver-based catalysts presents advantages from the economic point of view, due the low price of silver when compared to other noble metals, such as platinum or palladium. For this reason, scientific community have made a considerable effort in developing technologies based

on these materials. In the last years, Ag/Al_2O_3 catalysts have been widely studied as NO removal technology, in particular for diesel exhaust engines [3-6]. These studies have contributed to understand the nature and role of the different Ag species stabilised in the support, as well as the interaction with the different types of reductants, such as propylene, *n*-octane, toluene and hydrogen (among others).

Although Ag/Al_2O_3 catalysts have been evaluated by several authors as an interesting option when using long chain HC as reductants for HC-SCR [7, 8], Ag/zeolite catalysts have been far less studied.

Among the different zeolite structures, MFI is one of the most frequently considered for HC-SCR. Reports on Ag/MFI zeolites screening, Ag species characterisation and activity evaluation for HC-SCR with CH_4 [9-11], C_3H_6 [12-15] and C_3H_8 [16-18] can be found in the literature. However, only Čapek *et al.* [19] have applied Ag/MFI zeolites for HC-SCR reaction with long chain HC molecules, like *n*-decane. For this reason, further studies considering such reductant may be pertinent in order to further understand the importance of zeolite-based systems as HC-SCR technologies.

Furthermore, these authors only reported the activity of one Ag/MFI zeolite with Ag/Al = 0.55, with neither characterising the Ag species present in the catalyst nor evaluating the effect of other parameters on the Ag species distribution and catalytic activity.

Moreover, in previous works we have already evaluated Ag/LTL zeolites for HC-SCR with *n*-decane [20], focusing on the effect of different K^+ and H^+ contents in the Ag species nature and distribution as well as comparing the nature of Ag species in MFI zeolites with other supports like Al_2O_3 or ceria-zirconia [21].

The main goal of the present work is the study of Ag/MFI zeolites for the HC-SCR reaction with *n*-decane as a model molecule. The Ag content and the presence of H^+ and Na^+ as co-cations were chosen as the two main parameters to evaluate the catalysts performance on C_{10}-SCR. For this purpose, an Ag content of 4 and 9 wt.% were chosen, the first one in line with our previous works and the second one in order to over-exchange the MFI zeolite with Ag.

2. Experimental

2.1. Catalysts preparation

Catalysts were prepared from CBV 5524G zeolite (NH_4MFI), supplied by Zeolyst, with Si/Al = 25 and Wessalith DAZ P zeolite (silicalite-1), supplied by Degussa, with Si/Al > 500.

NaMFI was obtained by ion-exchanging three times the NH_4MFI form with a 1 M $NaNO_3$ (Sigma-Aldrich) solution. Ion-exchange was carried out at 100 ºC under reflux for 1 h, using a ratio between the volume of solution and the catalyst weight (v/w) equal to 100 $mL.g^{-1}$. After the third ion-exchange the catalyst was washed with distilled water and dried overnight at 80 ºC. NaMFI zeolite was calcined under air flow (4 $L.h^{-1}.g^{-1}$), kept at 200 ºC for 2 h and at 500 ºC for 8 h.

Ag(4)-HMFI and Ag(4)-NaMFI were prepared by ion-exchanging three times NH_4MFI and NaMFI, respectively, with a 0.01 M $AgNO_3$ (Sigma-Aldrich) solution. Ion-exchange was carried out at room temperature for 24 h in the dark, to avoid Ag^+ reduction, using a ratio between the volume of solution and the catalyst weight (v/w) equal to 100 $mL.g^{-1}$. After each ion-exchange, catalysts were washed with distilled water and dried at 100 ºC overnight. Then, calcination was performed as previously described.

For Ag(4)-silicalite and for all catalysts containing 9 wt.% Ag, silver was introduced by incipient wetness impregnation (IWI). A silver nitrate (Sigma-Aldrich) solution, with an appropriate concentration, was used to obtain 4 and 9 wt.% Ag in the zeolites. The solution was added drop-wise to each zeolite sample, until their pore volume was completely filled. Accordingly, Ag-HMFI, Ag-NaMFI and Ag-silicalite were obtained from NH_4-MFI, NaMFI and silicalite, respectively. After IWI procedure, all catalysts were calcined under air flow (4 $L.h^{-1}.g^{-1}$), kept at 200 ºC for 2 h and at 500 ºC for 8 h. The plateau at 200 ºC was used in order to remove the water adsorbed on the supports. This is especially important on the case of the zeolite supports to avoid dealumination during the calcination process at high temperatures.

2.2. Catalysts characterisation

Ag, Na, Al and Si contents in the catalysts were determined by ICP analysis.

Catalysts were characterised by powder X-ray Diffraction (XRD), transmission electron microscopy (TEM), hydrogen temperature programmed reduction (H_2-TPR), *in situ* diffuse reflectance UV-Vis spectroscopy (DRS UV-Vis) and pyridine adsorption followed by Fourier transformed infrared spectroscopy (FTIR).

Powder XRD patterns of each catalyst were collected on a *Bruker D8 Advance* diffractometer equipped with a graphite monochromator and using Cu-K_α radiation. A step size of 0.02 º (2θ) and a step time of 12 s were employed during acquisition.

TEM was performed on a *JEOL JEM 2010* microscope (LaB6 cannon) operating at 200 kV. Prior to TEM, the samples were crushed and then dispersed without solvent on a carbon-coated copper TEM grid.

H_2-TPR experiments were performed on a *Micromeritics Auto-Chem II 2920*, using 80 mg of catalyst. The sample was pre-treated under flowing argon or air (flow rate of 25 mL min^{-1}) from room temperature to 250 ºC (10 ºC.min^{-1}), kept at 250 ºC for 1 h and then cooled to RT. The reduction process was carried out under a mixture of 5% H_2/Ar with a flow rate of 30 mL.min^{-1}, from RT to 900 ºC at a heating rate of 10 ºC.min^{-1}. The H_2 mixture was stabilised in by-pass of the reactor and was put into contact with the catalyst only at the beginning of the temperature ramp. Hydrogen consumption was measured with a TCD. Water was trapped in a dry ice trap.

DRS UV-Vis spectra were collected on a *Varian Cary 5000 UV-Vis-NIR* spectrophotometer (range 200-800 nm, scan rate - 600 nm/min, data interval - 1 nm, SBW - 4 nm). A *Praying Mantis* accessory was used, coupled with a reaction chamber, in order to perform an oxidation treatment similar to the one described elsewhere [20]. Reflectance spectra were converted into the Schuster-Kubelka-Munk (SKM) function, F(R), calculated at each wavelength using the expression:

$$F(R) = \frac{(1-R)^2}{2R} \quad (2)$$

R is the ratio of the intensity of the light reflected by the sample to the one reflected by a standard (*Spectralon*®)

Pyridine adsorption followed by Fourier transform infrared (FTIR) spectroscopy was performed on a *Thermo Nicolet Nexus 670* spectrometer equipped with a DTGS detector (400-4000 cm^{-1}, 64 scans, 4 cm^{-1} resolution). Each catalyst was pressed into thin wafers (5–10 $mg.cm^{-2}$) and pre-treated in an *in-situ* infrared cell, under secondary vacuum (10^{-6} torr) at 450 ºC for 3 h. After the pre-treatment, a spectrum was recorded and, then, the sample was cooled down to 150 ºC and saturated with pyridine vapour (2 torr), for 10 min. Pyridine excess was removed for 30 min under secondary vacuum (10^{-6} torr), after which a spectrum was recorded. Before each spectrum collection, a background spectrum was always recorded.

2.3. Catalytic tests

Catalytic tests were performed in a tubular *pyrex* reactor using 170 mg of catalyst (dry basis), using the same apparatus described elsewhere [20].

Before the reaction, a pre-treatment was performed consisting in heating the catalyst under argon flow (15 $L.h^{-1}$), from room temperature until 500 ºC (5 $ºC.min^{-1}$) and keeping this temperature for 1 h, in order to clean the catalyst surface. Afterwards, the reactor was cooled to 300 ºC still under argon flow. Meanwhile, the reaction mixture was stabilised in by-pass. When it was stable, the reaction mixture was fed to the reactor. Once the signals were stable, the temperature was raised 50 ºC and kept constant until the signals were stable again. This procedure was repeated until 500 ºC. NO_x SCR tests were performed using a mixture of 250 ppm NO, 150 ppm *n*-decane and 7 vol.% O_2 in flowing argon (total flow rate of 250 $mL.min^{-1}$).

The reactor outflow was continuously analysed. NO and NO_2 concentrations were detected by a Thermo 42C chemiluminescence analyser and CO, CO_2 and N_2O concentrations were detected by an ABB EL 3020 infrared analyser. A Pfeiffer Vacuum GSD 301 mass spectrometer (MS) was also used to follow the reaction, namely, the mass fragments corresponding to *n*-decane (m/z = 57, 71 and 85).

3. Results and Discussion

3.1. Chemical analysis

Chemical analysis shows that NaMFI has a Na^+ exchange level of 76% (Table 1). This means that despite the three Na^+ exchanges performed on NH_4MFI, there are still some NH_4^+ sites on the sample, which generate protonic sites on NaMFI after calcination.

For Ag(4)-HMFI and Ag(4)-NaMFI catalysts, the result from the addition of Ag/Al and Na/Al values is lower than the unity, which means that both catalysts also contain H^+ as compensating cations of Al^- in the zeolite framework. However, both Ag(9)-HMFI and Ag(9)-NaMFI catalysts present an Ag/Al ratio > 1 which means that both catalysts are over-exchanged. This means that, for these catalysts, H^+ may eventually not be present as a compensating cation, depending on the Ag species of the samples. The presence of H^+ in these catalysts will be analysed in next section.

Table 1 – Chemical composition of the catalysts.

Catalyst	Ag (wt.%)	Na (wt.%)	Ag/Al	Na/Al	H/Al [a)]
NaMFI	-	1.1	-	0.76	0.24
Ag(4)-HMFI	4.1	-	0.62	-	0.38
Ag(4)-NaMFI	4.3	0.23	0.65	0.16	0.19
Ag(4)-silicalite	4.3	-	-	-	-
Ag(9)-HMFI	8.8	-	1.40	-	n.d.
Ag(9)-NaMFI	9.6	1.0	1.55	0.76	n.d.
Ag(9)-silicalite	9.0	-	-	-	-

a) Theoretical value calculated using the formula: H/Al = 1 – (Ag/Al + Na/Al)

3.2. Pyridine adsorption followed by Fourier transform infrared spectroscopy (FTIR)

In order to evaluate the presence of H^+ and quantify the different types of acid sites (Lewis or Brønsted) present on the Ag-based catalysts, pyridine adsorption followed by FTIR spectroscopy was used. After pyridine adsorption at 150 ºC, the spectral bands around 1450

cm^{-1} (Lewis acid sites - LAS) and 1540 cm^{-1} (Brønsted acid sites - BAS) were integrated, taking into account the assumptions considered in a previous work [21]. Moreover, it should be noted that the presence of Ag^+ species on Ag-exchanged zeolites leads to an increase on the number of LAS at the expense of the number of BAS, due to H^+ replacement by Ag^+ on the zeolite exchange-sites [21, 22], which act like Lewis centres. Therefore, this technique is also an interesting tool for identification of the Ag species since it targets specifically Ag^+ species and is not able to identify other Ag species.Figure 1A and B illustrate the concentration of acid sites for both series of Ag-catalysts containing 4 and 9 wt.% Ag, respectively.

In first place, it can be seen that Ag(4)-HMFI and Ag(4)-NaMFI exhibit a similar amount of LAS, which correspond to Ag^+ species. This seems to hint that both catalysts have a similar amount of these species, which is in line with the similar H_2-TPR profiles and DRS UV-Vis spectra of Ag(4)-HMFI and Ag(4)-NaMFI, as it will be presented hereafter in sections 3.5 and 3.6.

Regarding the number of BAS on Ag(4)-HMFI and Ag(4)-NaMFI, they are much lower than the amount of LAS, which is in line with the replacement of protonic sites with Ag^+ species, as previous mentioned in this section. It is worth mentioning that Ag(4)-HMFI has a higher number of Brønsted sites than Ag(4)-NaMFI, which was already expected *a priori* by the presence of Na^+ on the latter catalyst. However, it should also be stated that even after Ag^+ ion-exchange, Ag(4)-NaMFI retained some Brønsted acidity, which implies that Ag^+ exchanges preferentially with Na^+ cations rather than with H^+ [23].

Concerning Ag(4)-silicalite acidity, the low number of LAS and the absence of Brønsted acidity is in line with the high Si content (Si/Al > 500) of the silicalite support. Moreover, the absence of Ag^+ species in Ag(4)-silicalite also agrees with the low amount of Lewis sites in this catalyst.

Among the catalysts containing 9 wt.% Ag, Ag(9)-HMFI contains the higher number of LAS. On the other hand, both Ag(9)-NaMFI and Ag(9)-silicalite have a number of LAS close to zero. This suggests that Ag(9)-HMFI has a significantly higher amount of Ag^+ species which is in line with H_2-TPR and DRS UV-Vis results shown in sections 3.5 and 3.6, respectively. Furthermore, Ag(9)-HMFI has a higher quantity of LAS compared to Ag(4)-HMFI (689 μmol/g *vs*. 585 μmol/g). This implies that Ag(9)-HMFI contains a greater amount of Ag^+ species comparatively to Ag(4)-HMFI. Furthermore, it is also worth mentioning that the increase in the number of LAS from

Ag(4)-HMFI to Ag(9)-HMFI (+ 104 μmol/g) is in good agreement with the simultaneous decrease on the number of BAS which is also observed between these two catalysts (- 107 μmol/g).

Regarding Ag(9)-NaMFI, this catalyst presents a low amount of LAS, suggesting a low amount of Ag^+ species in this catalyst (supporting H_2-TPR and DRS UV-Vis results). A low amount of BAS is also observed on this catalyst, which agrees with its high Na^+ exchange level (0.76, *vide* Table 1).

Lastly, Ag(9)-silicalite presents a similar acid sites distribution to that of Ag(4), which can be explained using a similar reasoning.

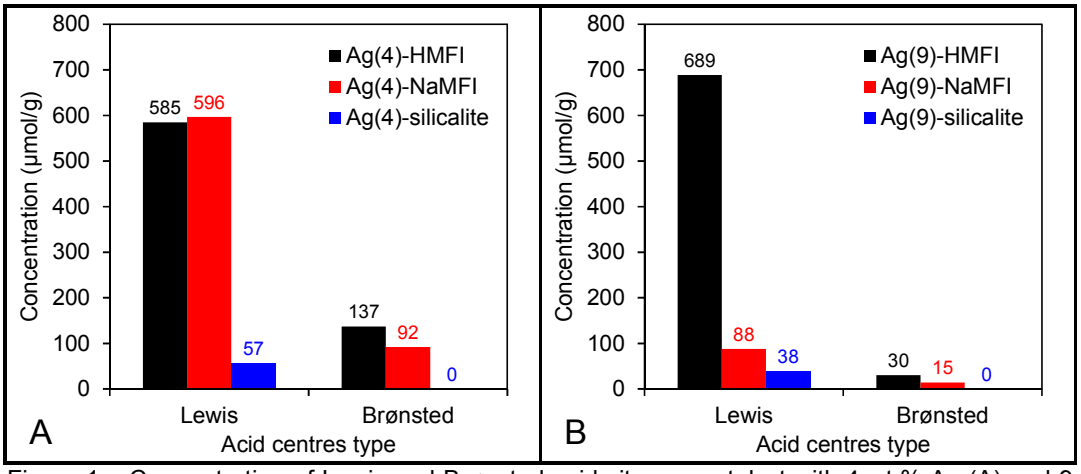

Figure 1 – Concentration of Lewis and Brønsted acid sites on catalyst with 4 wt.% Ag (A) and 9 wt.% Ag (B).

3.3. Powder X-ray diffraction (XRD)

Powder XRD patterns of all Ag-catalysts containing 4 and 9 wt.% Ag are presented in Figure 2A and B, respectively.

For the catalysts with lower Ag loading, only Ag(4)-silicalite presents metallic silver species (Ag^0), evidenced by the diffraction peaks at 2θ = 38.1, 44.3, 64.5 and 77.3º. However, for the catalysts containing 9 wt.% Ag, Ag^0 particles were identified in the three catalysts.

It is worthwhile mentioning that, for Ag(9)-silicalite, a considerably intense diffraction peak is observed at 2θ = 21.8º. This peak is also observed in Ag(4)-silicalite diffractogram, though its

intensity is significantly lower. It can be attributed to Cristobalite (ICDD 01-076-0941), a different SiO_2 phase from the silicalite support, which can be related to a possible desilication process. As it is documented in the literature [24] exposing the zeolite structure to an alkaline solution may lead to desilication of the zeolite framework. The pH of the $AgNO_3$ solution used in the IWI procedure during Ag-silicalite preparation was approximately 8.5. Though the solution is weakly alkaline, the fact that the silicalite support has a high Si content (Si/Al > 500) should facilitate the zeolite desilication [25].

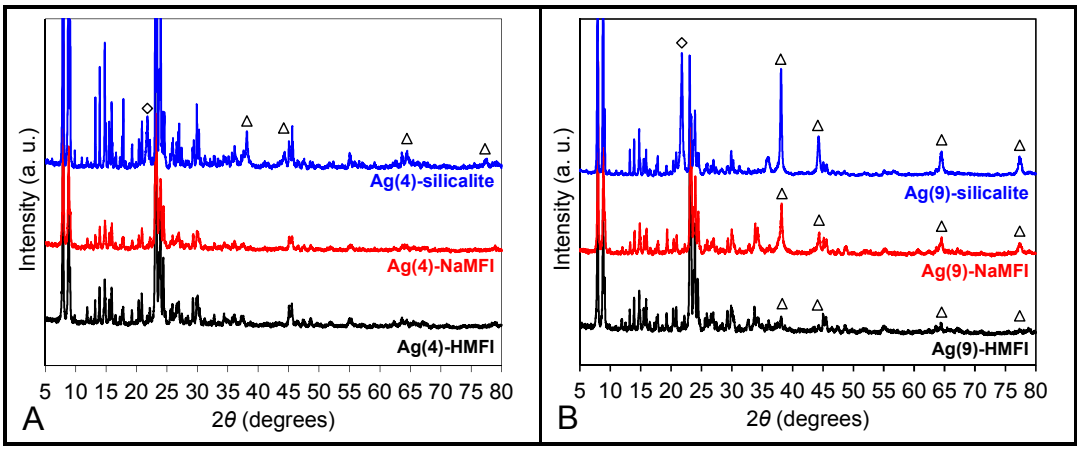

Figure 2 – Powder XRD patterns of catalysts with 4 wt.% Ag (A) and 9 wt.% Ag (B). Symbol (Δ) represent the main diffraction peaks of Ag^0 (ICDD 01-087-0720) and symbol (◊) represents one of the cristobalite diffraction peaks (ICDD 01-076-0941).

3.4. Transmission electron microscopy (TEM)

Figure 3 illustrates representative TEM images of all catalysts and the respective histograms of particle size distribution.

Regarding the catalysts containing 4 wt.% Ag, both Ag(4)-HMFI and Ag(4)-NaMFI present a similar particle size distribution, with a mean particle diameter of about 2 nm and narrow particle size distribution (σ = 0.5). In a previous work conducted by the authors [20] using Ag-LTL catalysts with metal loadings of the same order (*ca.* 4 wt.%) and containing different amounts of H^+ and K^+ co-cations, it was concluded that the particle size distribution was not affected by the

presence of these two cations. This conclusion seems to apply to Ag-MFI catalysts containing 4 wt.% of silver and different amounts of H^+ and Na^+.

As for Ag(4)-silicalite, contrarily to Ag(4)-HMFI and Ag(4)-NaMFI, this catalyst has a significantly higher mean particle diameter ($\overline{d_p}$ = 7 nm *vs.* $\overline{d_p}$ = 2 nm) with a wider particle size distribution (σ = 2 nm vs σ = 0.5). This is in line with the fact that the silicalite support does not have exchange sites which would help stabilise Ag in a more dispersed state, *e.g.* as Ag^+ species.

Concerning the nature of the Ag particles detected by TEM on all the 4 wt.% Ag-based catalysts, given the fact that powder XRD evidenced the presence of Ag^0 species on Ag(4)-silicalite (*vide supra* section 3.3), it can be assumed that for this catalyst the Ag particles detected by TEM correspond to Ag^0 particles. On the other hand, since no Ag^0 diffraction peaks where observed for Ag(4)-HMFI and Ag(4)-NaMFI, then the nature of the Ag particles detected by TEM on these two catalysts was assessed by measuring their inter-reticular plane distances using high-resolution TEM (HRTEM). As a result, plane (111) of face-centred cubic metallic silver was found on both catalysts, while plane (200) was also found on Ag(4)-NaMFI. Evidence of crystallographic planes belonging to Ag_2O was not found. Therefore, it can be concluded that the Ag particles detected by TEM on Ag(4)-HMFI and Ag(4)-NaMFI also correspond to Ag^0 particles.

Regarding the catalysts containing 9 wt.% Ag, Ag(9)-HMFI has the same average particle size of Ag(4)-HMFI (2.0 nm) but with a significantly wider particle size distribution (σ = 0.9 *vs.* 0.5). This widening of the Ag particle size distribution is due to the presence of some higher diameter particles on Ag(9)-HMFI (> 5 nm). Although the population size of these higher diameter particles is not high enough to be statistically relevant to appear in the particle histogram of Ag(9)-HMFI, they are consistently present in some of Ag(9)-HMFI TEM micrographs (*e.g.* particles with about 10 nm can be seen in Figure 3). Furthermore, the presence of these higher diameter particles on Ag(9)-HMFI might explain the fact this catalyst exhibits diffraction peaks typical from metallic silver species, which were not detected on Ag(4)-HMFI. Concerning Ag(9)-NaMFI, comparatively to Ag(9)-HMFI, this catalyst exhibits not only significantly larger silver particles ($\overline{d_p}$ = 11 nm *vs.* $\overline{d_p}$ = 2.0 nm), but also presents a wide distribution (σ = 5 nm *vs.* σ =

0.9 nm). This result suggests that, for catalysts containing a high Ag loading (9 wt.% Ag), the presence of different co-cations (H^+ and Na^+) affects the formation of Ag particles, with the presence of Na^+ leading to the formation of greater Ag particles.

Regarding Ag(9)-silicalite, this catalyst presents slightly smaller particles than Ag(9)-NaMFI ($\overline{d_p}$ = 9 nm *vs.* $\overline{d_p}$ = 11 nm, respectively) but has a slightly wider particle size distribution (σ = 7 nm vs. σ = 5 nm, respectively).

Lastly, it should be noted that, given the fact that Ag^0 species were detected by powder XRD on all three of the catalysts containing 9 wt.% Ag (*vide supra* section 3.3), then it can be assumed that the Ag particles identified by TEM correspond to Ag^0 particles.

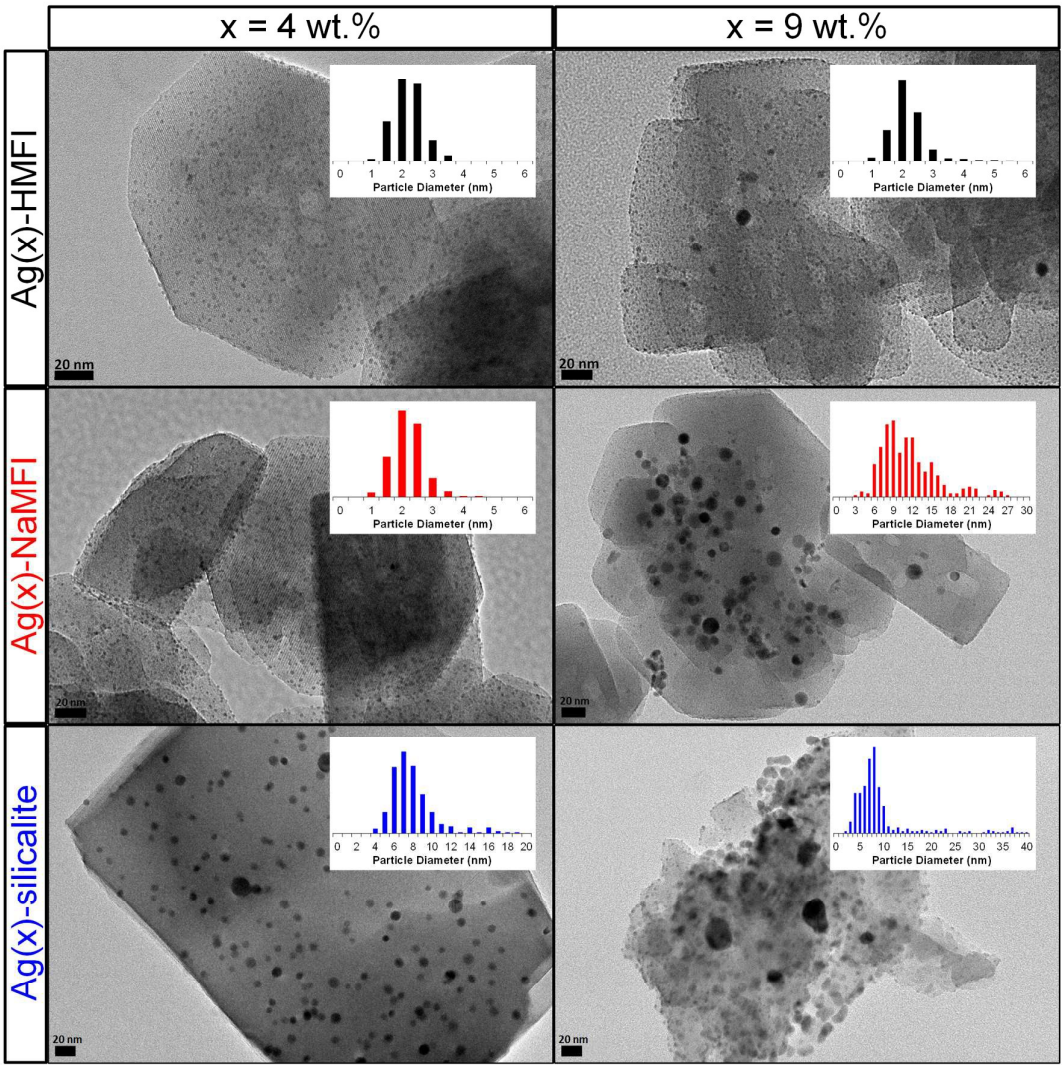

Figure 3 – TEM images and Ag particle size histograms of Ag-catalysts containing 4 and 9 wt.% Ag.

Table 2 – Average particle diameter $\overline{d_p}$ and respective standard deviation (σ).

Catalyst	$\overline{d_p}$ (nm)	$\pm\sigma$ (nm)
Ag(4)-HMFI	2.0	0.5
Ag(4)-NaMFI	1.9	0.5
Ag(4)-silicalite	7	2
Ag(9)-HMFI	2.0	0.9
Ag(9)-NaMFI	11	5
Ag(9)-silicalite	9	7

3.5. Hydrogen temperature programmed reduction (H_2-TPR)

H_2-TPR profiles of Ag-catalysts containing 4 and 9 wt.% of silver are presented in Figure 4A and B, respectively.

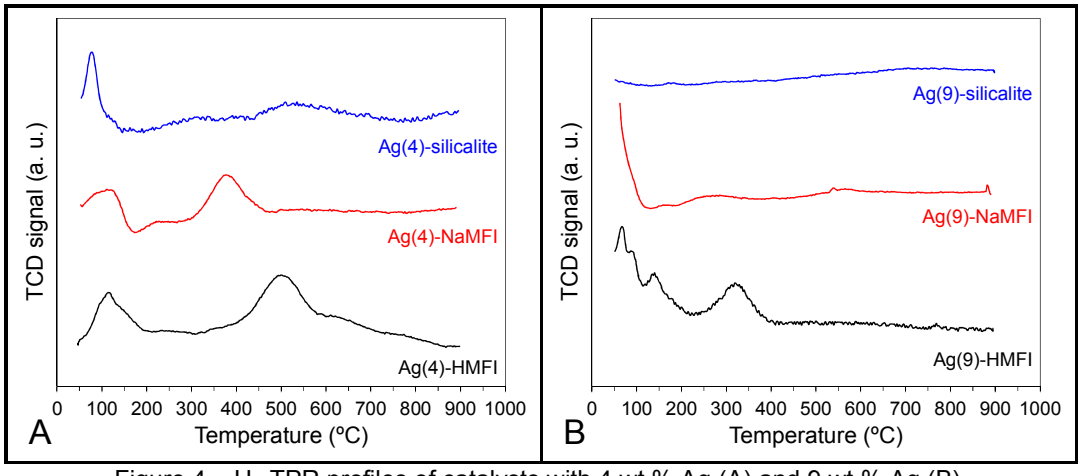

Figure 4 – H_2-TPR profiles of catalysts with 4 wt.% Ag (A) and 9 wt.% Ag (B).

Around 110 ºC, Ag(4)-HMFI and Ag(4)-NaMFI exhibit a peak attributed to the reduction of silver ions (Ag^+) into partially charged silver ion clusters ($Ag_n^{\delta+}$) [26]. Ag(4)-HMFI exhibits a second peak, around 500 ºC, which is ascribed to the reduction of $Ag_n^{\delta+}$ into metallic Ag clusters with

few Ag atoms (Ag_m) or metallic silver species (Ag^0) [27]. This reduction process also takes place in Ag(4)-NaMFI, but at lower temperature (around 385 ºC). This suggests that $Ag_n^{\delta+}$ are more stable when only H^+ is present as co-cation (instead of Na^+ and H^+), which can be attributed to the inhibition of reduction by the presence of protonic sites in the zeolites, shifting the equilibrium of the reduction process [28]. The shift of a reduction peak to lower temperatures when Na^+ is present in an Ag/zeolite catalyst was also observed by Berndt *et al*. [22]. For 5 wt.% Ag/MOR zeolites, when Na^+ was present as co-cation instead of H^+, the last reduction process detected by H_2-TPR shifted from 815 to 300 ºC. However, it should be noted that in addition to a change in the co-cation, the Si/Al ratio of the samples tested by Berndt *et al*. also differed by the double (10 *vs.* 5.6), which can also contribute to affect the reduction processes temperatures.

The H_2-TPR profile of Ag(4)-silicalite has only one main reduction peak with maximum at 80 ºC, signalling the presence of only one Ag oxidised species. Taking into account that the silicalite support does not have exchange-sites, the presence of oxidised Ag species with an ionic form on this zeolite, such as Ag^+ or $Ag_n^{\delta+}$ is highly unlikely. Therefore, the reduction peak on Ag(4)-silicalite must be attributed to one of the possible Ag oxides: AgO or Ag_2O. However, since AgO is a mixture of Ag_2O_3 and Ag_2O, it has two reduction processes. Therefore, the reduction peak on Ag(4)-silicalite can be attributed to Ag_2O [26].

From Figure 4B, one can see that the over-exchanged catalysts containing 9 wt.% Ag have distinct H_2-TPR profiles from the catalysts containing 4 wt.% Ag. On Ag(9)-HMFI, the two reduction processes that occur at low temperature (< 100 ºC) can be tentatively ascribed to AgO reduction [26]. Furthermore, the reduction peak with maximum at 140 ºC (also present on Ag(4)-HMFI) can be attributed to Ag^+ reduction to $Ag_n^{\delta+}$, while the reduction peak occurring at 325 ºC can be ascribed to $Ag_n^{\delta+}$ reduction to Ag_m or Ag^0 [27].

Ag(9)-NaMFI presents a H_2-TPR profile entirely distinct from that of Ag(9)-HMFI. While Ag(9)-HMFI has several oxidised Ag species, Ag(9)-NaMFI seems to have only one H_2 consumption process starting from the beginning of the H_2-TPR experiment, which can be tentatively assigned to Ag_2O reduction [26]. Clearly, the presence of Na^+ in this over-exchanged zeolite induces the formation of much easier reducible Ag species when compared with Ag(9)-HMFI catalyst.

Finally, no reduction processes can be observed in the H_2-TPR profile of Ag(9)-silicalite, suggesting that all silver is stabilised as Ag_m or Ag^0, which is in line with both the absence of exchange sites on the silicalite support and with the higher silver loading in this catalyst compared to Ag(4)-silicalite.

3.6. Diffuse reflectance UV-Vis spectroscopy (DRS UV-Vis)

Diffuse reflectance UV-Vis spectra of Ag-zeolites containing 4 and 9 wt.% Ag are represented in Figure 5A and B, respectively.

Both Ag(4)-HMFI and Ag(4)-NaMFI exhibit three bands at 215, 265 and 309 nm. The first band is assigned to the presence of silver ion species (Ag^+) [29] and the latter two bands can be ascribed to $Ag_n^{\delta+}$ [27] and Ag_m [30], respectively.

As for Ag(4)-silicalite, its spectrum has two absorption bands, at 260 and 405 nm. According to literature, the first band can be attributed to either $Ag_n^{\delta+}$ [31] or Ag_m [16, 30]. However, since Ag(4)-silicalite does not have exchange-sites, it should not be able to stabilise cationic species, like $Ag_n^{\delta+}$. Therefore, the band at 260 nm can be ascribed to Ag_m species. As for the second band, at 405 nm, it can be ascribed to Ag^0 particles [16, 32], also detected by powder XRD analysis (*vide supra* section 3.3).

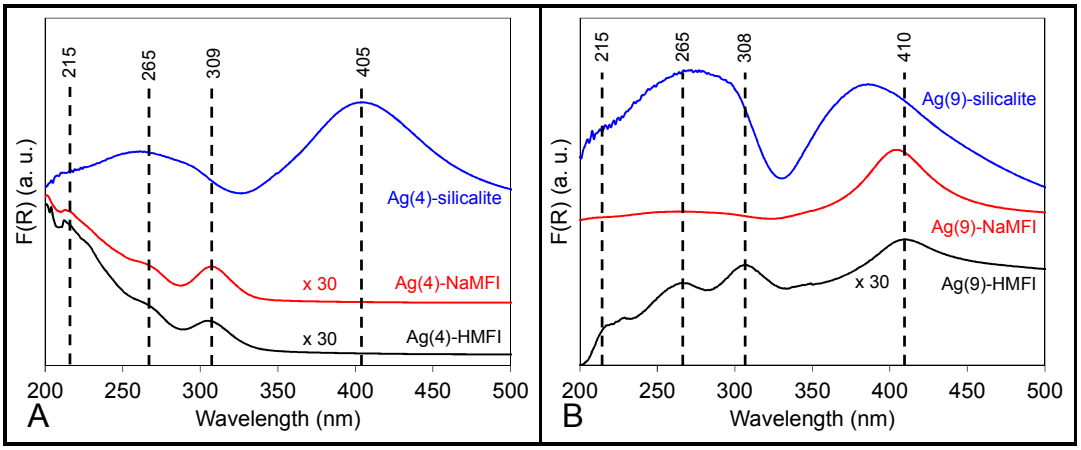

Figure 5 – DRS UV-Vis spectra of Ag-zeolites with 4 wt.% Ag (A) and 9 wt.% (B), at RT after heating the samples up to 500 ºC under air flow.

Regarding the three 9 wt.% Ag-containing catalysts (Figure 5B), unlike the case of Ag(4)-HMFI and Ag(4)-NaMFI which had rather similar spectra, Ag(9)-HMFI and Ag(9)-NaMFI have completely different spectra. Therefore, it seems that the presence of Na^+ in the zeolite support has a greater impact in the Ag species distribution when the zeolite support is over-exchanged with Ag.

Concerning Ag(9)-HMFI spectrum, four absorption bands can be observed at 215, 265, 308 and 410 nm, which can be attributed to Ag^+ [29], $Ag_n^{\delta+}$ [27], Ag_m [30] and Ag^0 [33], respectively. When comparing Ag(9)-HMFI and Ag(4)-HMFI spectra, the main difference is the presence of Ag^0 species on Ag(9)-HMFI. Therefore, it seems that over-exchanging an HMFI(25) zeolite with Ag leads to the formation reduced Ag species, which have an oxidation state lower than +1. This would be expected *a priori*, since the available zeolite exchange-sites are not enough to stabilise all Ag introduced as Ag^+ (theoretical exchange level of 1.4).

As for Ag(9)-NaMFI, DRS UV-Vis spectrum of this catalyst has a single band at 410 nm, attributed to Ag^0 species, which is also present on Ag(9)-HMFI. However, in the case of Ag(9)-NaMFI this band is much more intense, indicating a higher Ag^0 particles relative amount.

Finally, Ag(9)-silicalite spectrum is similar to that of Ag(4)-silicalite, presenting two bands at 265 and 385 nm, corresponding to Ag_m and Ag^0 species, respectively.

3.7. NO_x SCR with *n*-decane

The catalytic performance of Ag-zeolites containing 4 wt.% Ag is illustrated in Figure 6. It can be seen that Ag(4)-HMFI and Ag(4)-NaMFI have similar NO_x conversion into N_2 and N_2O profiles, with a maximum NO_x conversion into N_2 of about 50% at 500 ºC and a maximum NO_x conversion into N_2O of about 10% at 400 ºC. Regarding CO and CO_2 formation profiles, although up to 450 ºC these two profiles are identical for both catalysts, at 500 ºC Ag(4)-NaMFI presents a much lower CO formation (67 vs. 29%) and a higher CO_2 formation (33 vs. 66%). According to H_2-TPR and DRS UV-Vis results (Figure 4 and Figure 5, respectively), the presence of Na^+ as co-cation leads to a higher reducibility of partially charged silver ion clusters ($Ag_n^{\delta+}$) species. If these species lead to the formation of metallic silver particles (Ag^0) in Ag(4)-

NaMFI at 500 ºC, under reaction conditions, then the presence of these species could explain the differences between the two catalysts regarding CO and CO_2 formation.

Regarding Ag(4)-silicalite, from Figure 6, it can be concluded that it exhibits a poor performance for NO_x conversion into N_2. The maximum NO_x conversion into N_2 is 10%, at 400 ºC, while maximum NO_x conversion into N_2O is 15%, at 350 ºC. A low CO formation, reaching a maximum of 15%, at 400 ºC, can also be observed. In addition, CO_2 formation at 300 ºC is already 60% and stays above 80% between 350-500 ºC.

As evidenced by H_2-TPR and DRS UV-Vis, Ag(4)-silicalite possesses mainly reduced Ag_m and Ag^0 species, with a small amount of easily reducible Ag_2O. The presence of reduced Ag species can account for the high CO_2 selectivity. Moreover, it seems that the presence of Ag^+ and/or $Ag_n^{\delta+}$ species, which can be stabilised in the zeolite exchange-sites, are required in order for the catalyst to be active for the NO_x SCR reaction. This is in line with the some works that can be found in the literature, which claim that Ag^+ and $Ag_n^{\delta+}$ species are crucial for a good HC-SCR activity [21, 27, 34, 35].

Figure 7 presents the catalytic performance of Ag-zeolite catalysts with 9 wt.% Ag. Contrarily to what was observed for the corresponding catalysts with 4 wt.% Ag, it is possible to see that Ag(9)-HMFI and Ag(9)-NaMFI have different NO_x conversion into N_2 and into N_2O profiles. The maximum NO_x conversion into N_2 is about 30 % between 350-450 ºC over Ag(9)-HMFI, while over Ag(9)-NaMFI it is only 10%, at 440 ºC. NO_x conversion into N_2O, however, shows the opposite trend, with a greater amount of N_2O being formed over Ag(9)-NaMFI (maximum of 26% at 335 ºC vs. about 15% at 350 ºC). Hence, the presence of Na^+ as co-cation leads to a detrimental effect in total NO_x conversion and selectivity towards N_2. Concerning C_{10} conversion into CO and CO_2, for both catalysts, no CO formation is observed (100% selectivity towards CO_2). However, for Ag(9)-NaMFI, CO_2 light-off temperature is lower than that of Ag(9)-HMFI: at 280 ºC, C_{10} conversion into CO_2 is already 77% vs. about 10% at 300 ºC.

Given the fact that, according to these two catalysts characterisation, Na^+ presence leads to the formation of Ag^0 particles on Ag(9)-NaMFI in a greater amount than on Ag(9)-HMFI, at the expense of Ag^+ and $Ag_n^{\delta+}$ species, these results can explain the differences in NO_x and C_{10} conversion profiles between these two catalysts. The lower NO_x conversion into N_2 can be

explained by the absence of both Ag^{+} and $Ag_n^{\delta+}$ species on Ag(9)-NaMFI, while the higher N_2O and CO_2 formation can be explained by the presence of a greater amount of Ag^0 particles in this catalyst.

Finally, it is worthwhile to mention that Ag(9)-silicalite exhibits a similar catalytic performance to Ag(4)-silicalite. This performance is characterised by a low NO_x conversion into N_2 and a high CH_4 conversion into CO_2, which can be explained by the fact that both catalysts contain similar silver species, namely, Ag_m and Ag^0 species.

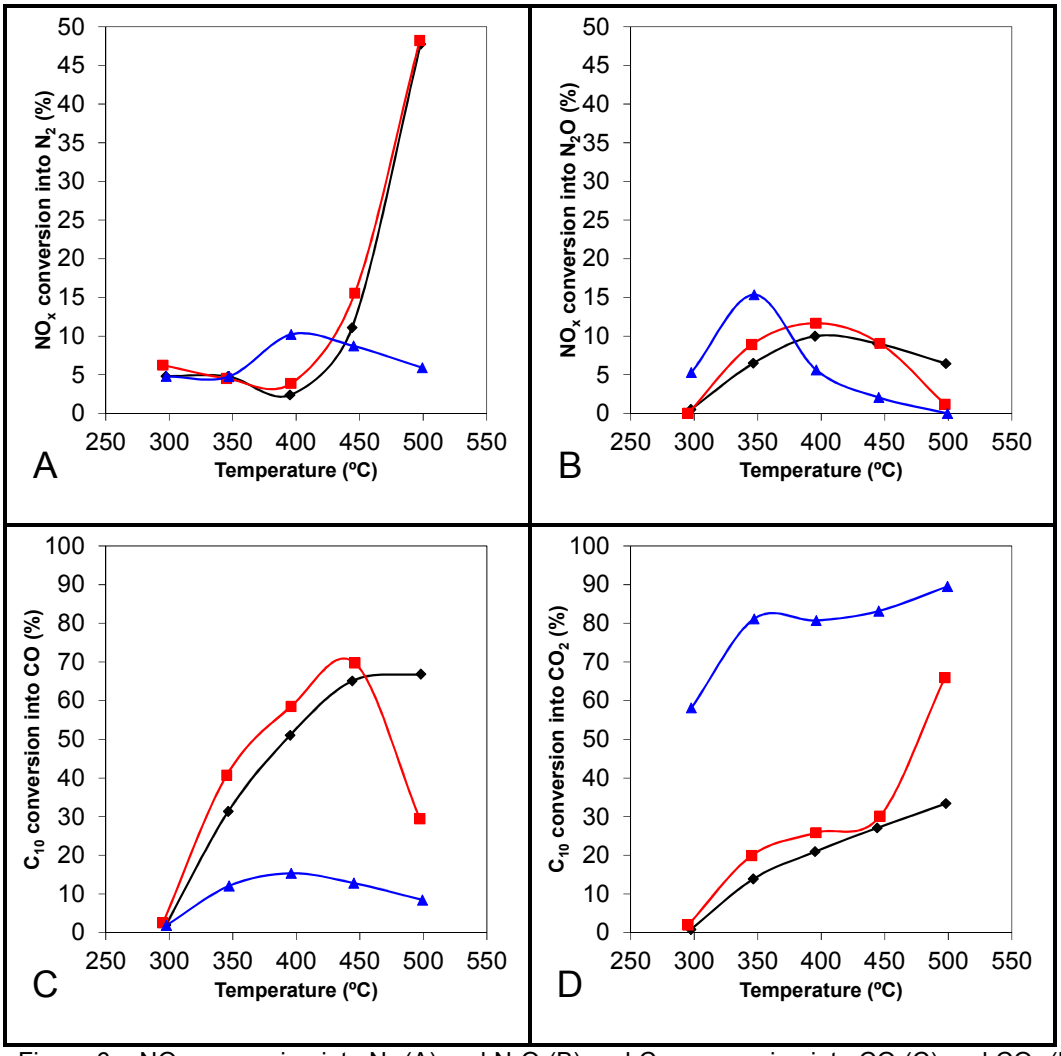

Figure 6 – NO_x conversion into N_2 (A) and N_2O (B) and C_{10} conversion into CO (C) and CO_2 (D) with 250 ppm NO, 150 ppm C_{10} and 7% O_2 over Ag(4)-HMFI (♦), Ag(4)-NaMFI (■) and Ag(4)-Silicalite (▲).

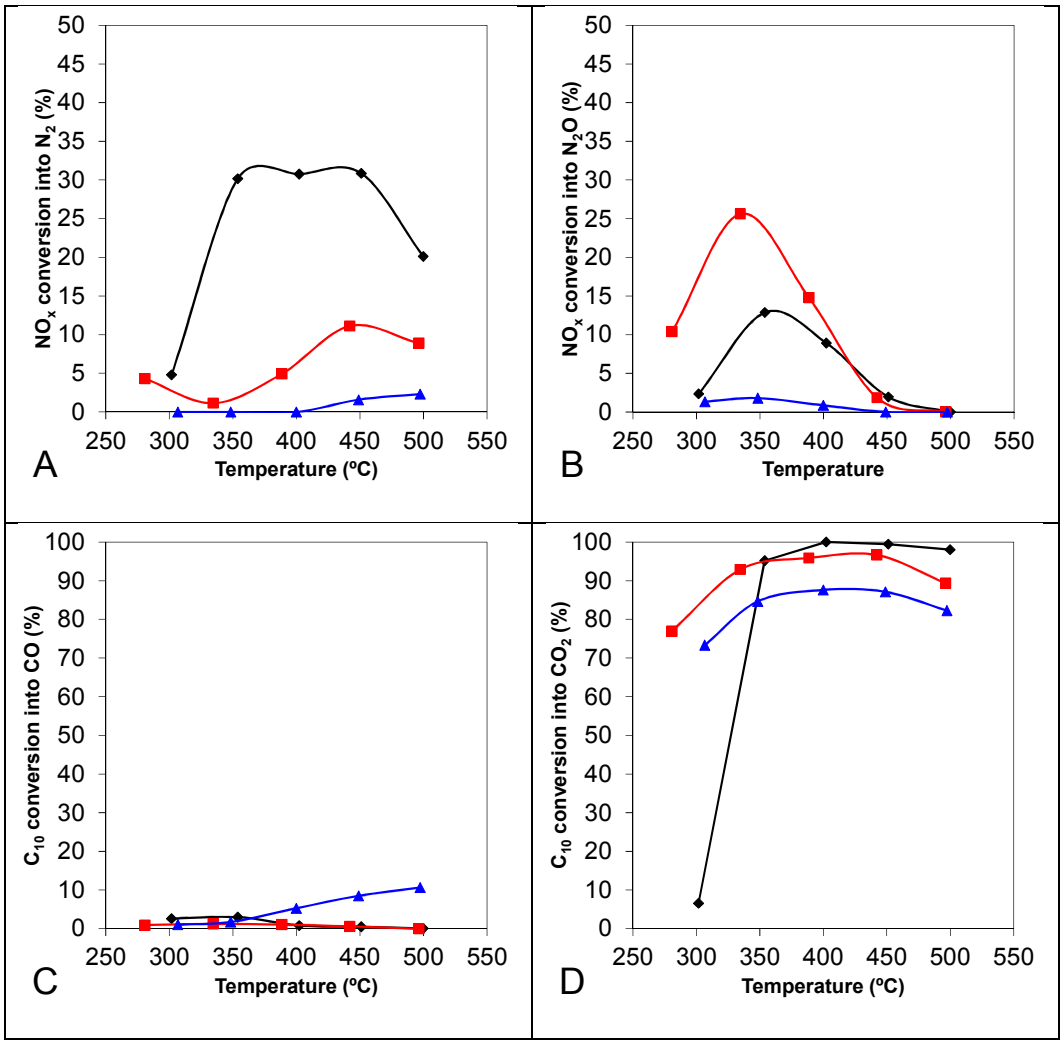

Figure 7 – NO_x conversion into N_2 (A) and N_2O (B) and C_{10} conversion into CO (C) and CO_2 (D) with 250 ppm NO, 150 ppm C_{10} and 7% O_2 over Ag(9)-HMFI (♦), Ag(9)-NaMFI (■) and Ag(9)-Silicalite (▲).

4. Conclusions

Two sets of catalysts, one containing 4 wt.% Ag and the other containing 9 wt.% Ag were evaluated in this work regarding the nature of the Ag species and their performance on NO_x C_{10}-SCR. In each set, the co-cation present was changed from only H^+ to H^+ and Na^+.

The effect of Na^+ presence as co-cation is highly dependent on the Ag content of the MFI zeolite support. For an Ag content of 4 wt.%, Na^+ presence does not have a significant impact on the Ag species distribution, although the $Ag_n^{\delta+}$ species reducibility is increased. The main Ag species present on Ag(4)-HMFI and Ag(4)-NaMFI are Ag^+ and $Ag_n^{\delta+}$. It has also been evidenced by pyridine adsorption followed by FTIR that the amount of Ag^+ species is the same on both catalysts. This is translated into a similar NO_x conversion profile for these two catalysts, with a maximum NO_x conversion into N_2 on the high temperature range (500 ºC).

An increase of the Ag content from 4 to 9 wt.% on MFI zeolite support containing only H^+ (Ag(4)-HMFI *vs.* Ag(9)-HMFI) leads to the appearance of reduced Ag species such as Ag_m and Ag^0, albeit the amount of Ag^+ species also increases. This translates in a shift of the maximum NO_x conversion into N_2 to the lower temperature range, *i.e.* from 500 ºC to 300-450 ºC.

On the other hand, contrarily to the MFI zeolite supports containing 4 wt.% Ag, Na^+ presence on MFI zeolites containing 9 wt.% Ag (over-exchanged catalysts) leads to a complete change in the Ag species distribution, with Ag^0 species becoming dominant. As consequence, NO_x conversion into N_2 severely decreases. This means that Na^+ presence has a negative effect due to the decrease in the amount of oxidised Ag species, namely Ag^+ and $Ag_n^{\delta+}$.

Regarding both Ag-containing catalysts prepared using silicalite support, regardless of the Ag content (4 or 9 wt.%), both catalysts contain only reduced Ag species, namely Ag_m and Ag^0 particles. Taking into account that they also show almost zero NO_x conversion into N_2 with a predominance of Ag^0 species, this seems to hint that the presence of exchange-sites on MFI zeolite support is critical to the presence and stabilisation of oxidised Ag^+ and $Ag_n^{\delta+}$ species, which lead to higher C_{10}-SCR activities.

Acknowledgements

The authors acknowledge Fundação para a Ciência e a Tecnologia (FCT) for financial support (grants number SFRH/BD/44108/2008, SFRH/BD/78639/2011 and SFRH/BPD/91397/2012 and projects PTDC/EQU-ERQ/102771/2008 and project UID/QUI/00100/2013).

References

1. European Union, Transport & Environment - Road Vehicles, http://ec.europa.eu/environment/air/transport/road.htm, (accessed June 2015, 2015).
2. P. Granger and V. I. Parvulescu, *Chem. Rev.*, 2011, **111**, 3155-3207.
3. K. Shimizu, K. Sawabe and A. Satsuma, *Catal. Sci. Technol.*, 2011, **1**, 331-341.
4. H. Kannisto, K. Arve, T. Pingel, A. Hellman, H. Harelind, K. Eranen, E. Olsson, M. Skoglundh and D. Y. Murzin, *Catal. Sci. Technol.*, 2013, **3**, 644-653.
5. K. Ralphs, C. D'Agostino, R. Burch, S. Chansai, L. F. Gladden, C. Hardacre, S. L. James, J. Mitchell and S. F. R. Taylor, *Catal. Sci. Technol.*, 2014, **4**, 531-539.
6. M. M. Aziz, H. Härelind and D. Creaser, *Catal. Sci. Technol.*, 2015, **5**, 296-309.
7. K. Arve, K. Eranen, M. Snare, F. Klingstedt and D. Y. Murzin, *Top. Catal.*, 2007, **42-43**, 399-403.
8. D. Y. Yoon, J.-H. Park, H.-C. Kang, P. S. Kim, I.-S. Nam, G. K. Yeo, J. K. Kil and M.-S. Cha, *Appl. Catal., B*, 2011, **101**, 275-282.
9. Z. Li and M. Flytzani-Stephanopoulos, *Appl. Catal., A*, 1997, **165**, 15-34.
10. C. Shi, M. Cheng, Z. Qu and X. Bao, *Appl. Catal., B*, 2004, **51**, 171-181.
11. C. Shi, M. Cheng, Z. Qu and X. Bao, *J. Mol. Catal. A: Chem.*, 2005, **235**, 35-43.
12. T. Furusawa, K. Seshan, J. A. Lercher, L. Lefferts and K.-i. Aika, *Appl. Catal., B*, 2002, **37**, 205-216.
13. K. A. Bethke and H. H. Kung, *J. Catal.*, 1997, **172**, 93-102.
14. G. B. F. Seijger, P. van Kooten Niekerk, K. Krishna, H. P. A. Calis, H. van Bekkum and C. M. van den Bleek, *Appl. Catal., B*, 2003, **40**, 31-42.
15. R. Wusirika, S. Ogunwumi and W. Lucas, *SAE Tech. Pap.*, 2005.
16. J. Shibata, Y. Takada, A. Shichi, S. Satokawa, A. Satsuma and T. Hattori, *J. Catal.*, 2004, **222**, 368-376.
17. K. Shimizu, K. Sugino, K. Kato, S. Yokota, K. Okumura and A. Satsuma, *J. Phys. Chem. C*, 2007, **111**, 6481-6487.
18. A. Satsuma, J. Shibata, K. Shimizu and T. Hattori, *Catal. Surv. Asia*, 2005, **9**, 75-85.
19. L. Capek, K. Novoveska, Z. Sobalik and B. Wichterlova, *Stud. Surf. Sci. Catal.*, 2005, **158**, 1993-2000.

20. R. Bartolomeu, R. Bertolo, S. Casale, A. Fernandes, C. Henriques, P. da Costa and F. Ribeiro, *Micropor. Mesopor. Mat.*, 2013, **169**, 137-147.

21. R. Bartolomeu, B. Azambre, A. Westermann, A. Fernandes, R. Bértolo, H. I. Hamoud, C. Henriques, P. Da Costa and F. Ribeiro, *Appl. Catal., B*, 2014, **150–151**, 204-217.

22. H. Berndt, M. Richter, T. Gerlach and M. Baerns, *J. Chem. Soc., Faraday Trans.*, 1998, **94**, 2043-2046.

23. J. Weitkamp and L. Puppe, in *Catalysis and Zeolites: Fundamentals and Applications.*, Springer-Verlag Berlin Heidelberg, Germany, 1999, ch. 3, pp. 81-197.

24. J. C. Groen, J. A. Moulijn and J. Perez-Ramirez, *J. Mater. Chem.*, 2006, **16**, 2121-2131.

25. J. C. Groen, L. A. A. Peffer, J. A. Moulijn and J. Perez-Ramirez, *Micropor. Mesopor. Mat.*, 2004, **69**, 29-34.

26. T. Nanba, S. Masukawa, J. Uchisawa and A. Obuchi, *J. Catal.*, 2008, **259**, 250-259.

27. J. Shibata, K. Shimizu, Y. Takada, A. Shichia, H. Yoshida, S. Satokawa, A. Satsuma and T. Hattori, *J. Catal.*, 2004, **227**, 367-374.

28. R. Bulanek, B. Wichterlova, Z. Sobalik and J. Tichy, *Appl. Catal., B*, 2001, **31**, 13-25.

29. R. Bartolomeu, C. Henriques, P. da Costa and F. Ribeiro, *Catal. Today*, 2011, **176**, 81-87.

30. Y. Kuroda, T. Mori, H. Sugiyama, Y. Uozumi, K. Ikeda, A. Itadani and M. Nagao, *J. Colloid. Interf. Sci.*, 2009, **333**, 294-299.

31. J. Shibata, Y. Takada, A. Shichi, S. Satokawa, A. Satsuma and T. Hattori, *Appl. Catal., B*, 2004, **54**, 137-144.

32. V. S. Gurin, V. P. Petranovskii, M. A. Hernandez, N. E. Bogdanchikova and A. A. Alexeenko, *Mater. Sci. Eng., A*, 2005, **391**, 71-76.

33. D. Chen, Z. Qu, S. Shen, X. Li, Y. Shi, Y. Wang, Q. Fu and J. Wu, *Catal. Today*, 2011, **175**, 338-345.

34. P. Sazama, L. Capek, H. Drobna, Z. Sobalik, J. Dedecek, K. Arve and B. Wichterlova, *J. Catal.*, 2005, **232**, 302-317.

35. K. Arve, L. Capek, F. Klingstedt, K. Eranen, L. E. Lindfors, D. Y. Murzin, J. Dedecek, Z. Sobalik and B. Wichterlova, *Top. Catal.*, 2004, **30-1**, 91-95.